Supporting Information

Overcoming thermodynamic incompatibilities with photons: multi-carbon hydrocarbons from methane and carbon dioxide *via* a hybrid photocatalytic dry reforming/Fischer–Tropsch process

Hiroaki Kaneko,[a] Shusaku Shoji,[b] Yohei Cho,[a,c] Tomotaka Sugimura,[a] Ayako Hashimoto,[d] Hideki Abe,[b] Akira Yamaguchi,[a] Masahiro Miyauchi*[a]

[a] Department of Materials Science and Engineering, School of Materials and Chemical Technology, Institute of Science Tokyo, 2-12-1 Ookayama, Meguro-ku, Tokyo 152-8552, Japan.

[b] National Institute for Materials Science, 1-1 Namiki, Tsukuba, Ibaraki 305-0044, Japan.

[c] Graduate School of Advanced Science and Technology, Japan Advanced Institute of Science and Technology, 1-1 Asahidai, Nomi, Ishikawa 923-1292, Japan.

[d] National Institute for Materials Science, 1-2-1 Sengen, Tsukuba, Ibaraki 305-0047, Japan.

Contents of Supporting Information

Note 1. Experimental details,

Synthesis of DRM catalyst; Rh/STO

A 200 mg mass of a commercial $SrTiO_3$ (≥ 99%, Sigma-Aldrich) was introduced into a 20 mL aqueous solution at 80 °C, in which 10.23 mg of $RhCl_3 \cdot 3H_2O$ (≥ 94%, Kanto Chemical) was dissolved. This solution was stirred continuously and dried to a powder at 70 °C overnight. The powder was treated at 500 °C under a 5% from of H_2 in Ar to reduce the Rh species. Subsequently, the powder form of Rh/STO was synthesised. The introduced amount of Rh into the impregnation process was 2.0 wt% versus $SrTiO_3$.

Synthesis of FTS catalyst; Co,Ru/SBA-15

A 200 mg mass of a commercial SBA-15 (≥ 99.9%, Sigma-Aldrich) was introduced into a 5 mL aqueous solution at 60 °C, in which 197.5 mg of $Co(NO_3)_2 \cdot 6H_2O$ (≥ 99.95%, Kanto Chemical) and 4.8 mg $RuCl_3 \cdot nH_2O$ (≥ 99.9%, Wako Pure Chemical Industries) was dissolved. This solution was stirred continuously and dried to a powder at 60 °C overnight. The powder was calcined in air at 450 °C for 8h. The introduced amount of Co and Ru into the impregnation process was 20 wt% and 1 wt% versus SBA-15, respectively.

Characterization of Rh/STO and Co,Ru/SBA-15

The microstructures of the catalysts were observed using TEM (JEOL, JEM-ARM200F and Hitachi High-Technologies, H7650 Zero.A) and SEM (JEOL, JCM-7000). The SEM apparatus was equipped with an energy-dispersive X-ray spectroscopy (EDS) for the elemental analysis. The crystal structure of the catalysts was evaluated using XRD (Rigaku, MiniFlex600-C). The amount of Rh, Co and Ru loaded on the STO or SBA-15 was measured by XRF (Malvern Panalytical, Epsilon1). The optical absorption properties of the catalysts were recorded using UV–vis DRS (JASCO, V-770). Nitrogen adsorption measurements at 77 K were performed on a volumetric adsorption analyzer (MICROMERITICS, TriStar II). Before the measurements, the samples were outgassed for 1 h in the degas port of the adsorption apparatus at 80 °C.

Evaluation of catalytic performances

Photocatalytic DRM reactions and thermal FTS reactions were performed under in a temperature/pressure-controlled gas flow chamber with a sapphire window (ST Japan, Heat Chamber Type-1000). (Fig. S1)

For DRM reaction, the Rh/STO powder (5 mg) was placed in a porous alumina cup in the reactor chamber, and the inner diameter of the ceramic cup was 5 mm. The catalyst was illuminated using

a 200 W Hg–Xe lamp (Hayashi-Repic, LA-410UV-5) or 500 W Xe lamp (Kenko Tokina, XEF-501S). Each light irradiance was 2.7 W cm^{-2} and 5.3 W cm^{-2}, measured using a spectral radiometer (USHIO, USR-45). The surface temperature of the light-irradiated catalyst was measured by a radiative thermometer (JAPANSENSOR, FLHX-TNE0090-0200B003-000) through the sapphire window of the chamber. For FTS reaction, the Co,Ru/SBA-15 powder (3 mg) was placed in a porous alumina cup in the reactor chamber. The piping beyond the chamber outlet was heated to 80 °C by a ribbon furnace to ensure that no liquid hydrocarbons remained in the piping. For successive DRM and FTS reactions, the Rh/STO catalyst was placed in the upstream chamber and the Co,Ru/SBA-15 catalyst was placed in the downstream chamber. The two chambers were connected in series at the same pressure and temperature. The upstream chamber was illuminated, while the downstream chamber was dark. Prior to the FTS and successive DRM and FTS reaction evaluations, the Co,Ru/SBA-15 was treated with 5% H_2 in Ar gas at 400 °C for 1h to reduce Co and Ru oxides. The composition of the input DRM and FTS gas were 0.9% CH_4 and 0.9% CO_2 in Ar and 2.4% H_2 and 2.4% CO in Ar. The flow rate of the introduced gas was 15 mL min^{-1}. The concentrations of the outlet gas (CH_4, CO_2, H_2 and CO) were evaluated using gas chromatography with a thermal conductivity detector (GC TCD; Agilent, 490 Micro GC). The concentrations of the C2 + hydrocarbon product were evaluated using gas chromatography with a flame ionization detector (GC FID; SHIMADZU, GC-2014 GC).

In situ DRIFTS analysis

The *in situ* DRIFTS measurement was performed during the light irradiation onto Rh/STO catalyst using a Fourier transform infrared spectrometer (JASCO, FT/IR-4X), equipped with a MCT (HgCdTe) detector. The resolution was 4 cm^{-1} and the iteration time was 100 for each measurement. The sample holder was a temperature-controlled gas flow chamber with a KBr window (ST Japan, Heat Chamber Type-1000). Mixture gas of CH_4 (4.5%) and CO_2 (4.5%) with Ar was introduced into the chamber at the flow rate at 10 mL min^{-1}, and the light irradiation was conducted using a 200 W Hg–Xe lamp or 500 W Xe lamp through a KBr window of the chamber. Background measurement was conducted in an Ar atmosphere at room temperature after treatment at 120 °C for 30 mins to remove adsorbates.

Note 2. Calculation method for thermodynamic equilibrium

Thermodynamic equilibrium was calculated using the Chemical Equilibrium with Applications program (CEA), developed by the Glenn Research Center of NASA. For the calculation, the temperature was set at 700 °C, and the pressure was set to 0.1–2 MPa under the same gas atmosphere as DRM experiment (CH_4:CO_2:Ar = 0.9:0.9:98.2).

Table S1. Comparison of the experimental conditions and activities involved in the combining of CH_4 reforming and the FTS reaction.

No.	Catalysts (upper: DRM, lower: FTS)	Inlet gas concentration	Pressure (MPa)	Temperature (°C)	Energy source	H_2/CO ratio	C2 + yield/STY*	Ref.
1	2wt%Rh/$SrTiO_3$, 20wt%Co,1wt%Ru/SBA-15	CO_2/CH_4/Ar = 0.9/0.9/98.2	2.0	280 (surface temp. = 647)	200 W Hg–Xe lamp, external heating	0.72	0.34%, 305 μmol g^{-1} h^{-1}	This work
2	NiMg/$Ce_{0.6}Zr_{0.4}O_2$ Co/SiO_2	LFG/air/steam = 1/0.56/0.36	0.3 2.0	770 250	external heating	0.49	13wt%	1
3	10wt%Ni_3Zn/SiO_2, 10wt%Fe_5K_2/SiO_2	$CH_4/CO_2/H_2O/N_2$/ Ar = 1/1/1/0.4/2	0.5	800 400	external heating	–	12wt%	2
4	7.5wt%Co_5Ni_{95}@SiO_2(500)	$CH_4/CO_2/H_2O/N_2$/ Ar = 2/1/1/1/5	0.1	178–1013	300 W Xe lamp (> 435 nm)	0.90	17.5 μmol h^{-1} (= 58.3 μmol g^{-1} h^{-1})	3
5	No catalyst	CH_4/CO_2 = 2/1	0.1	55–65	Plasma (5.5 kV)	1.3	13%	4

The upper part of same cells represents DRM conditions, while the lower part represents FTS conditions.

* C2 + yield = $\frac{\Sigma\, x \times moles\ of\ C_xH_y\ produced}{moles\ of\ CH_4\ inlet + moles\ of\ CO_2\ inlet}$ (%) or

$\frac{\Sigma\, mass\ of\ C_xH_y\ produced}{mass\ of\ CH_4\ inlet + mass\ of\ CO_2\ inlet}$ (wt%)

C2 + STY = $\frac{\Sigma\, moles\ of\ C_xH_y\ produced}{mass\ of\ catalyst \times reaction\ time}$ (μmol g^{-1} h^{-1})

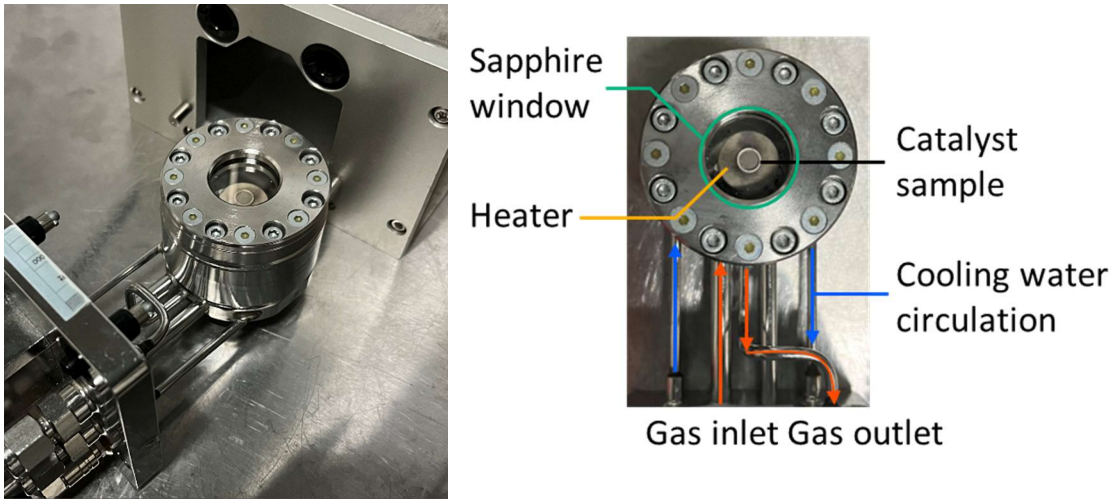

Figure S1. Photographs of a high-pressure durable gas flow chamber with a light transmission window.

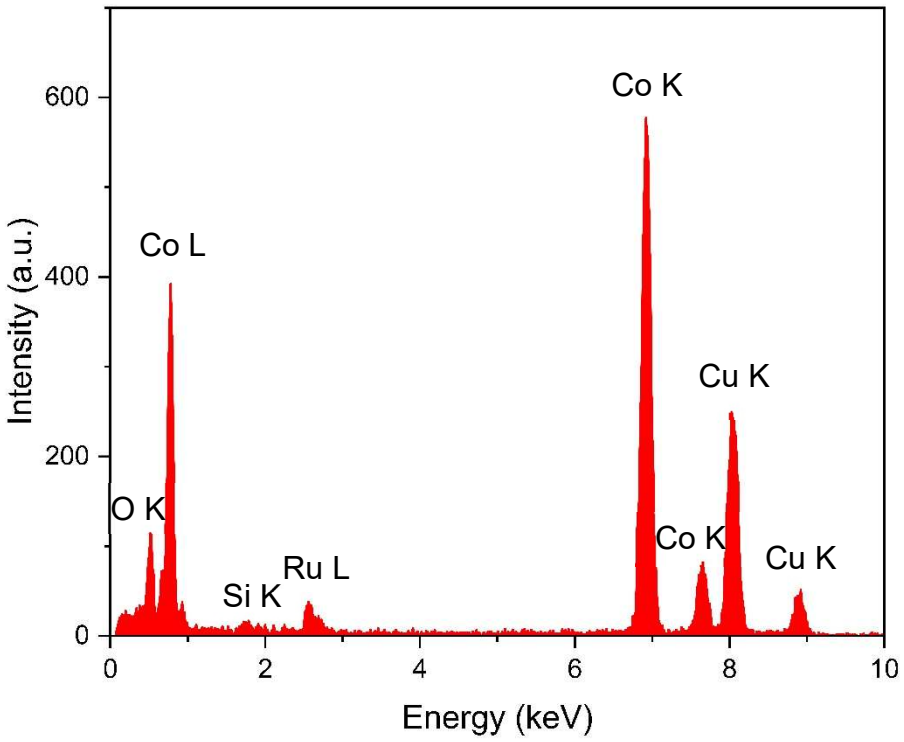

Figure S2. EDS spectrum of Co,Ru/SBA-15. Copper (Cu) signals originated in micro grids.

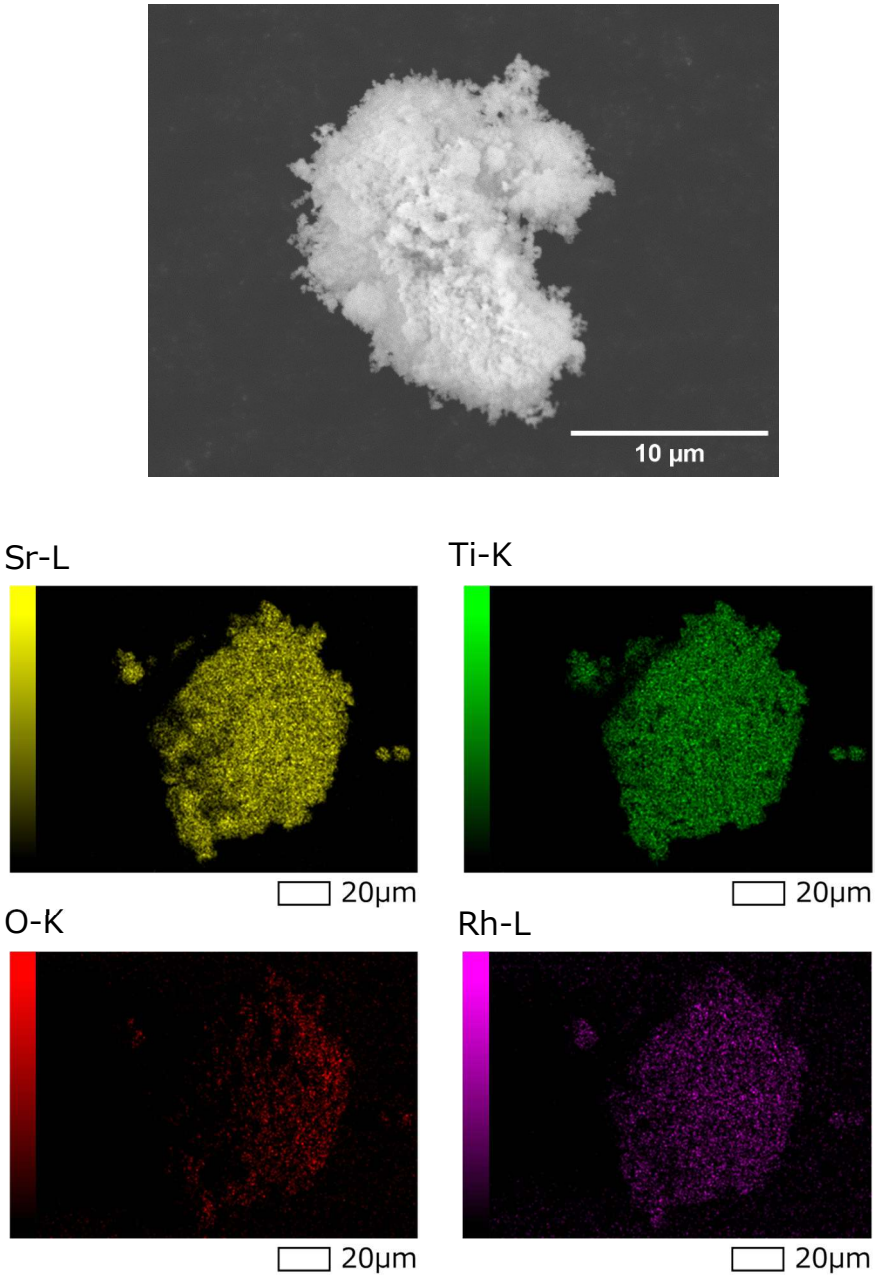

Figure S3. SEM image and its EDS elemental mapping images for strontium (Sr), titanium (Ti), oxygen (O), and rhodium (Rh) of Rh/STO, respectively.

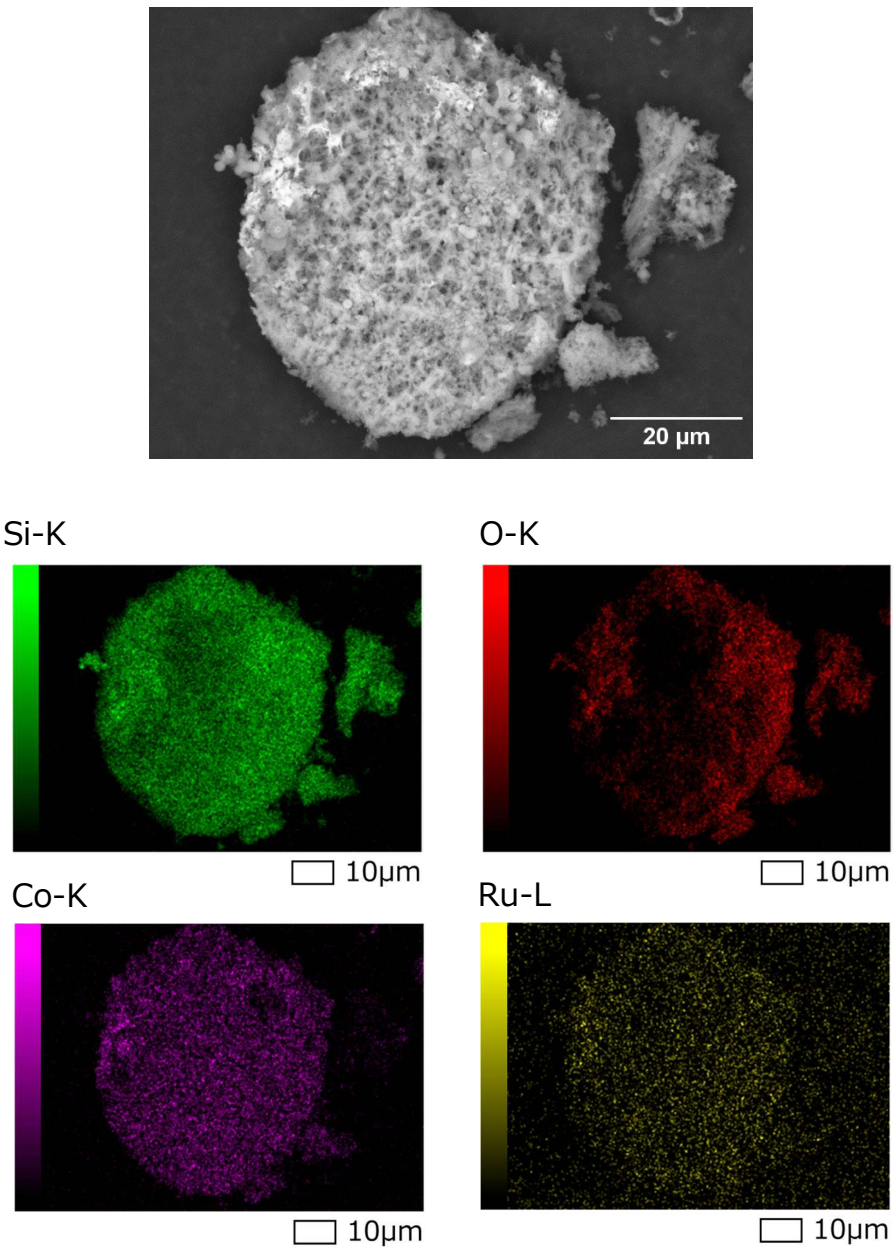

Figure S4. SEM image and its EDS elemental mapping images for silica (Si), oxygen (O), cobalt (Co), and ruthenium (Ru) of Co,Ru/SBA-15, respectively.

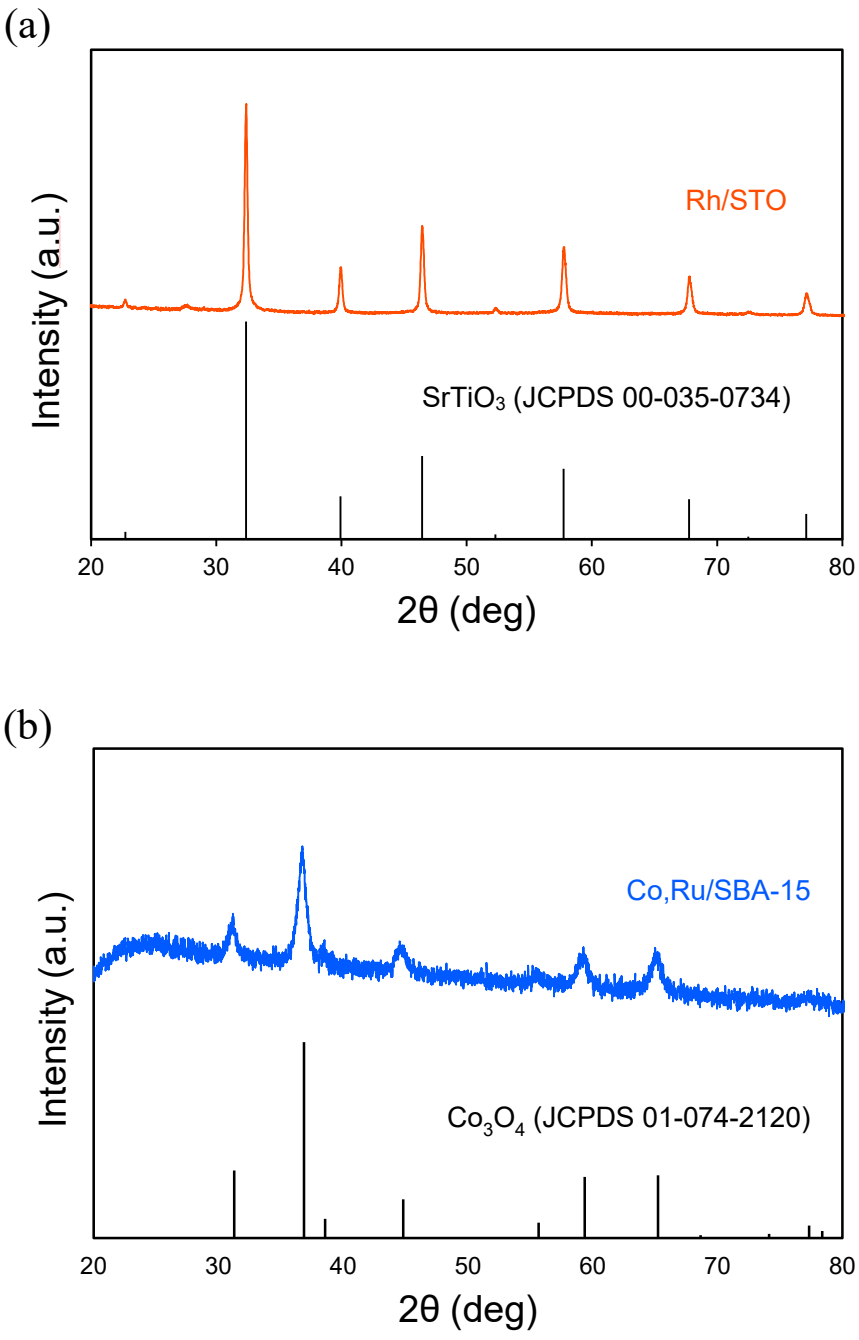

Figure S5. XRD patterns of (a) Rh/STO and (b) Co,Ru/SBA-15.

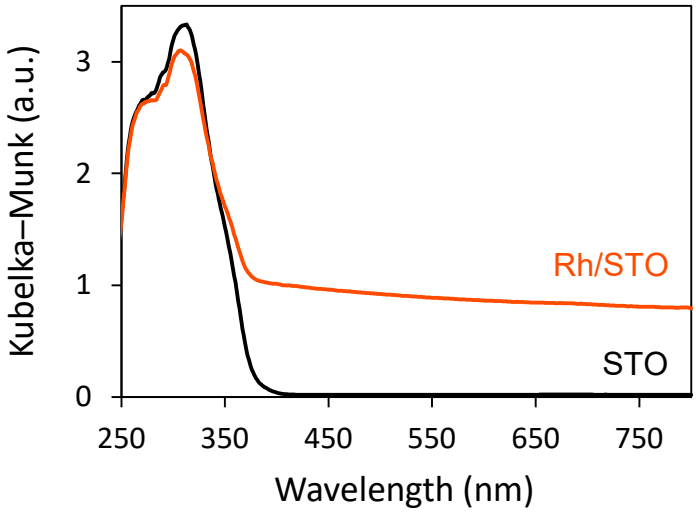

Figure S6. UV–vis DRS spectra of STO and Rh/STO.

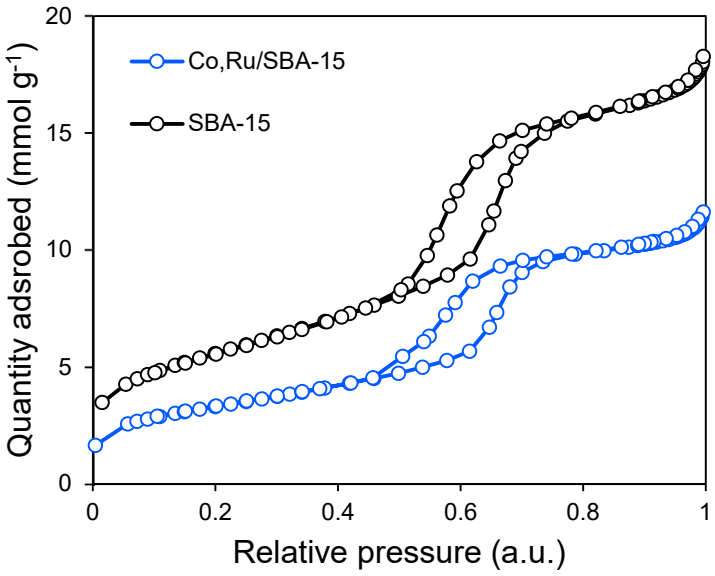

Figure S7. N_2 adsorption isotherms of SBA-15 and Co,Ru/SBA-15.

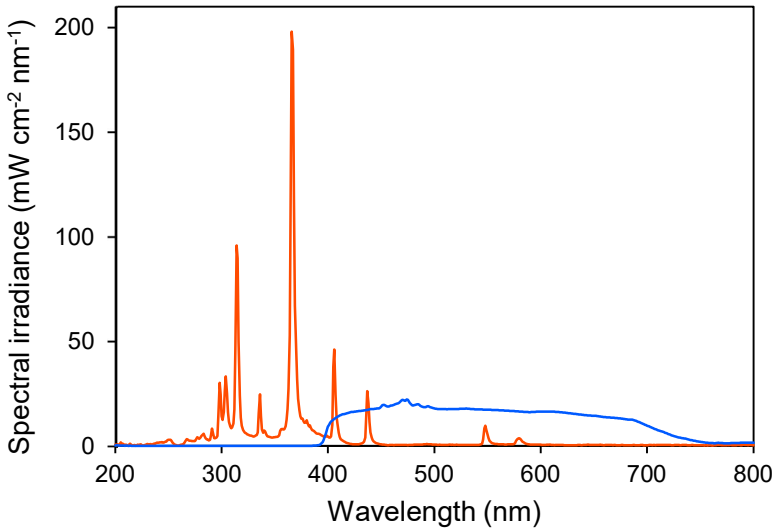

Figure S8. Spectral irradiance of a Hg–Xe lamp (red line) and Xe lamp with a long-pass cut-off filter below 400 nm (blue line). The irradiance was 2.7 W cm^{-2} for a Hg–Xe lamp and 5.3 W cm^{-2} for a Xe lamp.

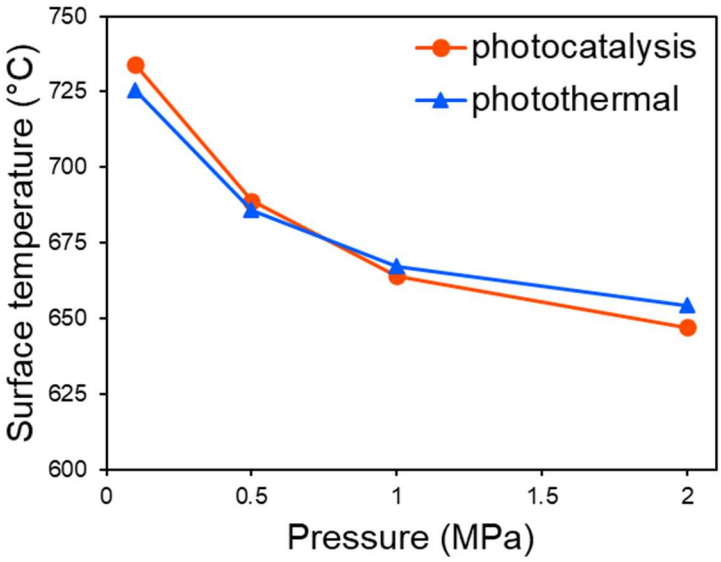

Figure S9. Surface temperature of Rh/STO during the photocatalytic and photothermal reaction.

The surface temperature of Rh/STO catalyst decreased slightly as pressure increased though the light intensity remained unchanged. This is because higher-pressure gases can absorb more energy from the light-irradiated catalyst surface.

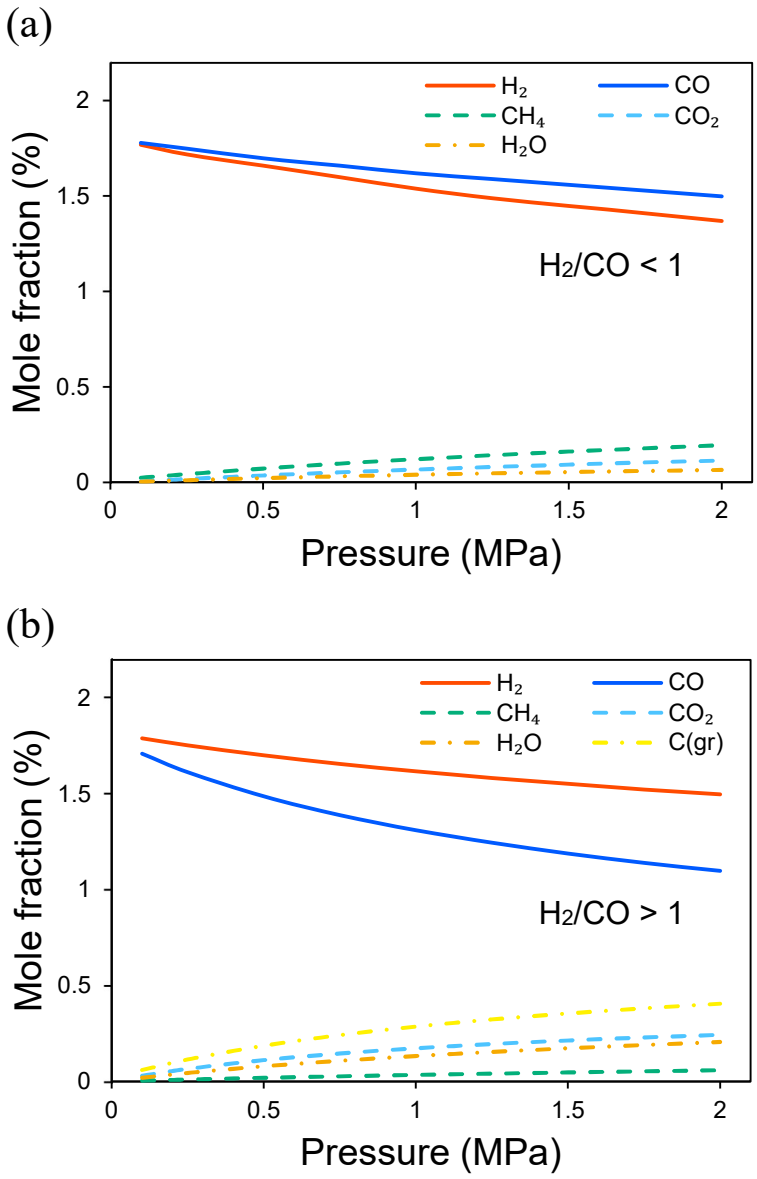

Figure S10. Pressure dependence on the thermodynamic equilibrium of DRM. The calculations are performed under the following conditions:(a) graphite carbon (C(gr)) was excluded from the calculation; (b) C(gr) was included in the calculation.

The H_2/CO ratio was below 1 in DRM reaction under UV and visible light irradiation conditions (Fig. 2 (a)). These trends are consistent with the thermodynamic equilibrium when solid carbon is excluded from the calculation (Fig. S10 (a)). This indicates that Rh/STO has anti-coking effects, as reported in previous studies.[5,6]

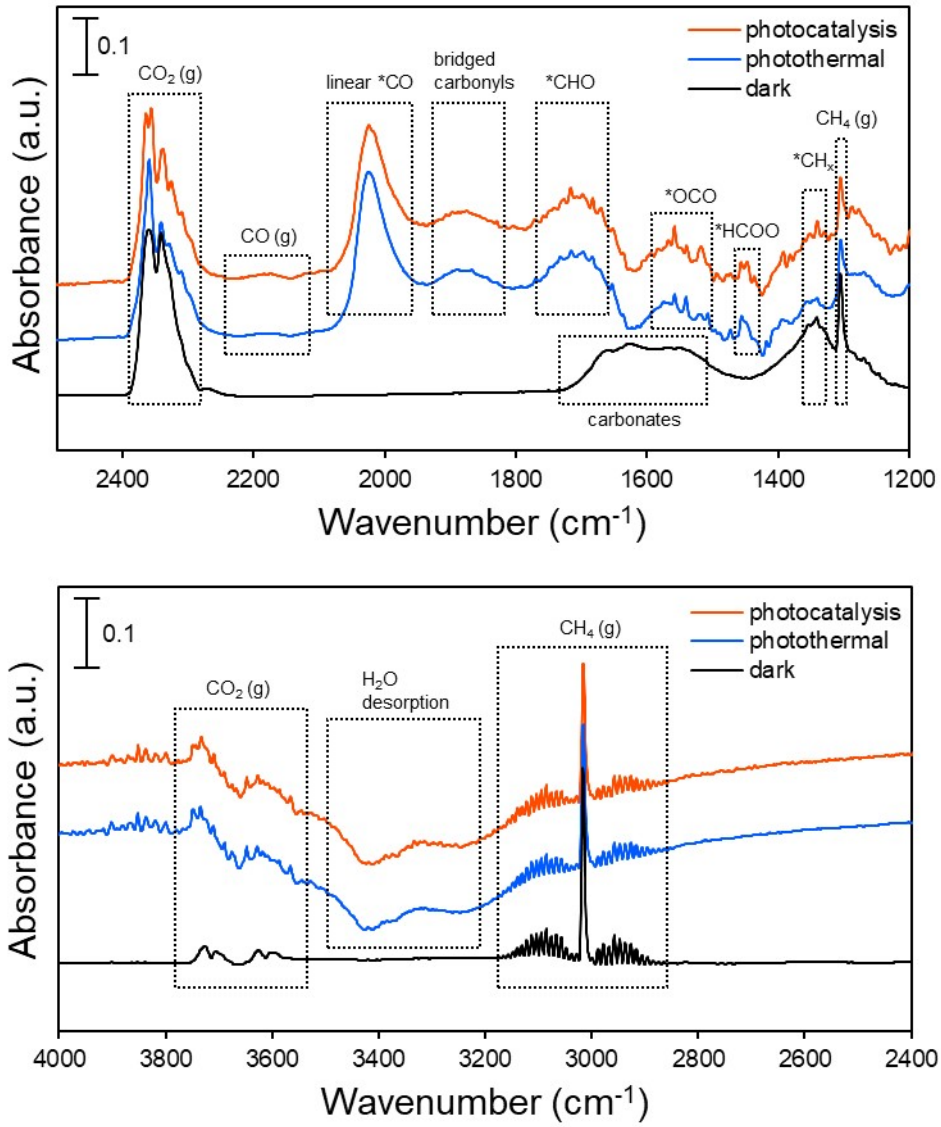

Figure S11. *In situ* DRIFTS spectra in the dark or under UV (photocatalysis), or visible (photothermal) light irradiation. The experiments were conducted in a flow of the relatively concentrated DRM gas (4.5% CH_4 and CO_2 in Ar) at room temperature.

Under dark condition, multiple IR peaks of *CH_x (1355 cm^{-1} and 1342 cm^{-1})[7] and carbonate species (1664 cm^{-1}, 1625 cm^{-1}, 1540 cm^{-1})[7] were observed. Also, an increase in gaseous CO (2174 cm^{-1}) and a decrease in gaseous CO_2 (2360 $cm^{-1}$and 2340 cm^{-1}) and CH_4 (3017 cm^{-1} and 1304 cm^{-1}) were observed, which is consistent with the experimental results of DRM reaction under light irradiation. H_2O desorption was caused by the increase in surface temperature under light irradiation.

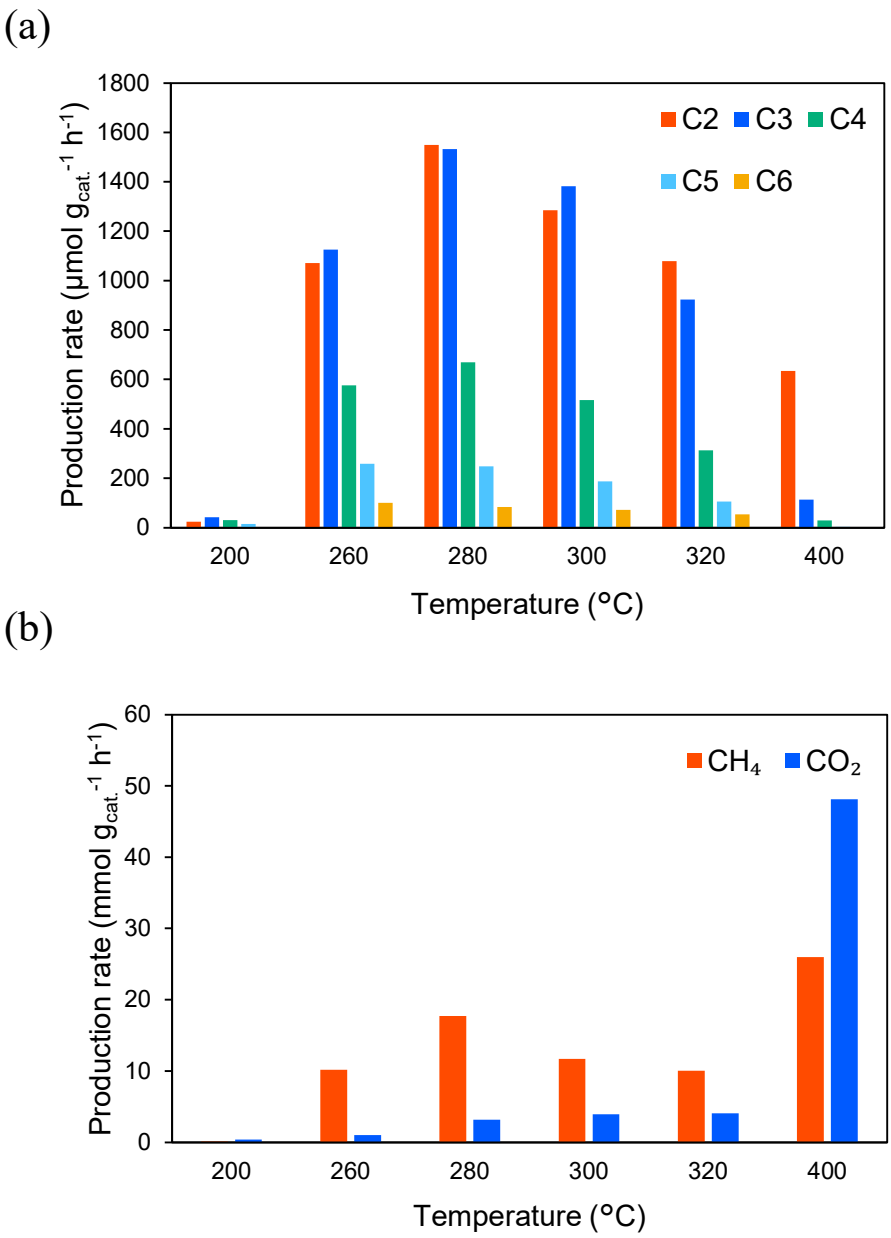

Figure S12. Production rates of (a) C2–C6 hydrocarbons and (b) CH_4 and CO_2 at 2.0 MPa. Sample: 3mg Co,Ru/SBA-15, heater set temperature: 200–400 °C, reactant gas composition: H_2:CO:Ar = 2.4:2.4:95.2 (volume ratio), and standard gas flow rate: 15 mL min^{-1}, respectively.

References in Supporting Information

1 X. Zhao, A. Naqi, D. M. Walker, T. Roberge, M. Kastelic, B. Joseph and J. N. Kuhn, *Sustain. Energy Fuels*, 2019, **3**, 539–549.

2 O. Johnson, Y. He, B. Joseph and J. N. Kuhn, *Energy Fuels*, 2025, **39**, 7815–7829.

3 H. A. El-Naggar, H. Asanuma, H. Yoshida and A. Yamamoto, *Sol. RRL*, 2025, **9**, 2500021.

4 D. Li, V. Rohani, F. Fabry, A. P. Ramaswamy, M. Sennour and L. Fulcheri, *Appl. Catal. B Environ.*, 2020, **261**, 118228.

5 S. Shoji, X. Peng, A. Yamaguchi, R. Watanabe, C. Fukuhara, Y. Cho, T. Yamamoto, S. Matsumura, M.-W. Yu, S. Ishii, T. Fujita, H. Abe and M. Miyauchi, *Nat. Catal.*, 2020, **3**, 148–153.

6 H. Kaneko, Y. Cho, T. Sugimura, A. Hashimoto, A. Yamaguchi and M. Miyauchi, *Chem. Commun.*, 2024, **60**, 10406–10409.

7 Z.-Y. Zhang, T. Zhang, R.-K. Wang, B. Yu, Z.-Y. Tang, H.-Y. Zheng, D. He, T. Xie and Z. Hu, *J. Catal.*, 2022, **413**, 829–842.